Mineralogical Magazine, October 2015, Vol. 79(5), pp. 1111–1121

Antipinite, $KNa_3Cu_2(C_2O_4)_4$, a new mineral species from a guano deposit at Pabellón de Pica, Chile

Nikita V. Chukanov[1,*], Sergey M. Aksenov[2,3], Ramiza K. Rastsvetaeva[3], Konstantin A. Lyssenko[4], Dmitriy I. Belakovskiy[5], Gunnar Färber[6], Gerhard Möhn[7] and Konstantin V. Van[8]

[1] Institute of Problems of Chemical Physics, Russian Academy of Sciences, Chernogolovka, Moscow region, 142432 Russia
[2] Faculty of Geology, St Petersburg State University, University Embankment 7/9, St Petersburg, 199034 Russia
[3] Institute of Crystallography, Russian Academy of Sciences, 59 Lenin Avenue, Moscow, 117333 Russia
[4] Institute of Organoelement Compounds, Russian Academy of Sciences, Vavilova Street 28, Moscow, 119991 Russia
[5] Fersman Mineralogical Museum of the Russian Academy of Sciences, Leninsky Prospekt 8-2, Moscow, 117071 Russia
[6] Bornsche Strasse 9, 39326 Samswegen, Germany
[7] Dr J. Wittemannstrasse 5, 65527 Niedernhausen, Germany
[8] Institute of Experimental Mineralogy, Russian Academy of Sciences, Chernogolovka, Moscow Region, 142432 Russia

[*Received 15 December 2014; Accepted 27 January 2015; Associate Editor: P. Leverett*]

ABSTRACT

The new oxalate mineral antipinite is found in a guano deposit located on the Pabellón de Pica Mountain, Iquique Province, Tarapacá Region, Chile. Associated minerals are halite, salammoniac, chanabayaite, joanneumite and clays. Antipinite occurs as blue, imperfect, short prismatic crystals up to 0.1 mm × 0.1 mm × 0.15 mm in size, as well as their clusters and random aggregates. The mineral is brittle. Mohs hardness is 2; D_{meas} = 2.53(3), D_{calc} = 2.549 g cm^{-3}. The infrared spectrum shows the presence of oxalate anions and the absence of absorptions associated with H_2O molecules, C–H bonds, CO_3^{2-}, NO_3^- and OH^- ions. Antipinite is optically biaxial (+), α = 1.432(3), β = 1.530(1), γ = 1.698(5), $2V_{meas}$ = 75(10)°, $2V_{calc}$ = 82°. The chemical composition (electron-microprobe data, C measured by gas chromatography of products of ignition at 1200°C, wt.%) is Na_2O 15.95, K_2O 5.65, CuO 27.34, C_2O_3 48.64, total 99.58. The empirical formula is $K_{0.96}Na_{3.04}Cu_{2.03}(C_{2.00}O_4)_4$ and the idealized formula is $KNa_3Cu_2(C_2O_4)_4$. The crystal structure was solved and refined to R = 0.033 based upon 4085 unique reflections with $I > 2\sigma(I)$. Antipinite is triclinic, space group $P\bar{1}$, a = 7.1574(5), b = 10.7099(8), c = 11.1320(8) Å, α = 113.093(1), β = 101.294(1), γ = 90.335(1)°, V = 766.51(3) Å^3, Z = 2. The strongest reflections of the powder X-ray diffraction pattern [d, Å (I,%) (hkl)] are 5.22 (40) (1$\bar{1}$1), 3.47 (100) (0$\bar{3}$2), 3.39 (80) ($\bar{2}$10), 3.01 (30) (0$\bar{3}$3, 220), 2.543 (40) (122, 0$\bar{3}$4, $\bar{1}$04), 2.481 (30) ($\bar{2}$13), 2.315 (30) (1$\bar{4}$3, $\bar{3}$10), 1.629 (30) (1$\bar{4}$6, $\bar{4}$ $\bar{1}$4, $\bar{2}$43, $\bar{1}$60).

Keywords: antipinite, new mineral, oxalate, crystal structure, guano, Pabellón de Pica, Chile.

Introduction

The mountain of Pabellón de Pica belongs to a belt of Late Paleozoic and Mesozoic igneous rocks stretching along the northern coast of Chile and bearing numerous bird guano deposits. Some details of the geological setting and the history of guano deposit development in the Tarapacá region are published elsewhere (Ericksen, 1981; Pankhurst and Hervé, 2007; Appelton and Notholt, 2002; Bojar *et al*., 2010). The guano deposit located on Pabellón de Pica is the type locality of several other N-bearing and organic minerals, ammineite, $CuCl_2(NH_3)_2$ (Bojar *et al*., 2010), joanneumite,

* E-mail: nikchukanov@yandex.ru
DOI: 10.1180/minmag.2015.079.5.07

FIG. 1. Aggregate of antipinite crystals on halite. Field of view: 0.7 mm. Photograph: M. Burkhardt.

$Cu(C_3N_3O_3H_2)_2(NH_3)_2$ (Bojar and Walter, 2012), chanabayaite, $Cu_4(N_3C_2H_2)_4(NH_3)_4Cl_2(Cl,OH)_2 \cdot H_2O$ (Chukanov *et al*., 2013) and shilovite, $Cu(NH_3)_4(NO_3)_2$ (Chukanov *et al*., 2014*b*). The new oxalate mineral antipinite, $KNa_3Cu_2(C_2O_4)_4$, was found by two of us (GF and GM) in the same guano deposit. The mineral and its name were approved by the Commission on New Minerals, Nomenclature and Classification (CNMNC) of the International Mineralogical Association (IMA 2014-027; Chukanov *et al*., 2014*a*). The type specimen is deposited in the collections of the Technische Universität, Bergakademie Freiberg, Germany, inventory number 83870. The new mineral is named in memory of Mikhail Yuvenal'evich Antipin (1951–2013), a specialist in the crystallography and crystal chemistry of organometallic and coordination compounds. He was awarded the Prize of the Russian Academy of Sciences for these investigations. He also investigated minerals especially studying electron density distribution. M.Y. Antipin was the head of the laboratory where the crystal structure of antipinite was first solved.

Occurrence, general appearance and physical properties

Antipinite occurs in the guano deposit situated in the lower part of the steep northern slope of Pabellón de Pica Mountain, 1.5 km south of Chanabaya village, Iquique Province, Tarapacá

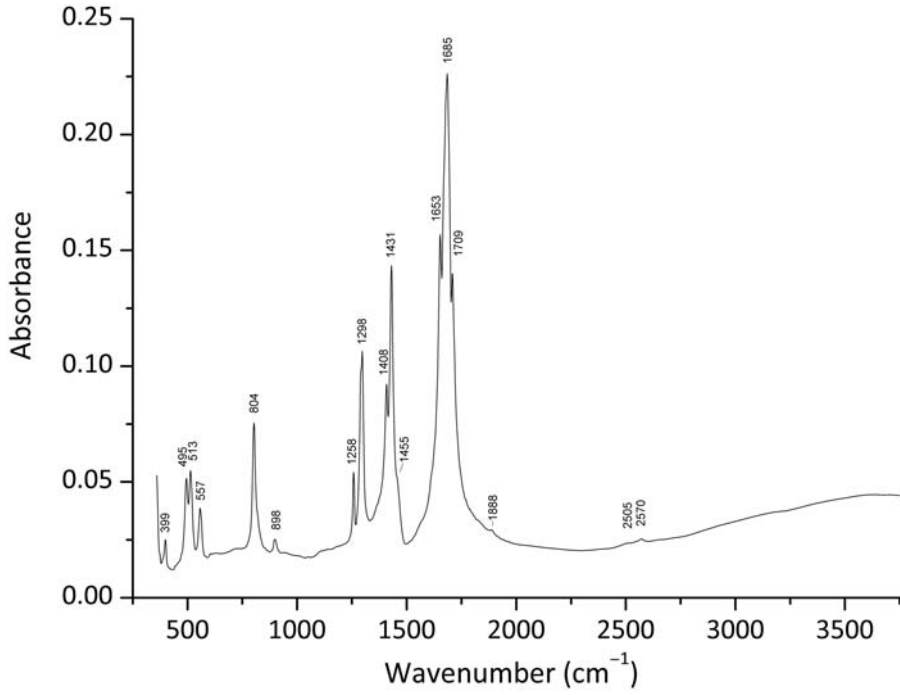

FIG. 2. The powder IR absorption spectrum of antipinite.

TABLE 1. Analytical results for antipinite (mean of 5 spot analyses).

Constituent (element)	Content, wt.%	Range	Standard deviation	Constituent (oxide)	Content, wt.%	Probe standard
Na	11.83	11.42–12.24	0.34	Na_2O	15.95	Albite
K	6.35	5.97–6.95	0.35	K_2O	7.65	Sanidine
Cu	21.84	21.34–22.18	0.46	CuO	27.34	$CuFeS_2$
C	16.22			C_2O_3	48.64	
Total	56.24				99.58	

TABLE 2. Powder X-ray diffraction data for antipinite.*

I_{meas}	d_{meas}	I_{calc}**	d_{calc}**	*hkl*	I_{meas}	d_{meas}	I_{calc}**	d_{calc}**	*hkl*
40	5.22	30	5.26	1 $\bar{1}$ 1	20	2.090	7	2.104	$2\bar{4}2$
							5	2.100	$\bar{2}40$
							8	2.084	$\bar{2}14$
100	3.47	80	3.44	$0\bar{3}2$	10	2.067	4	2.078	222
80	3.39	60	3.39	$\bar{2}10$	20	1.989	6	2.003	213
							2	1.989	$0\bar{4}5$
							2	1.984	$3\bar{2}2$
30	3.01	5	3.02	$0\bar{3}3$	10	1.831	6	1.838	312
		7	2.98	220			4	1.832	$1\bar{3}6$
20	2.96	7	2.98	$\bar{2}20$	20	1.794	3	1.803	$\bar{2}42$
		4	2.94	$\bar{2}\bar{2}1$			3	1.791	$\bar{1}51$
							2	1.788	$\bar{4}01$
30	2.86	14	2.90	$\bar{2}12$	20	1.774	3	1.779	$0\bar{6}2$
		14	2.90	$2\bar{2}1$			2	1.776	$0\bar{5}3$
		2	2.87	130			2	1.775	124
							2	1.767	$\bar{3}\bar{4}2$
20	2.77	7	2.80	031	10	1.728	3	1.728	$0\bar{6}1$
		5	2.80	211					
		17	2.74	220					
20	2.691	6	2.691	$\bar{2}\bar{2}3$	10	1.707	5	1.708	$2\bar{2}5$
							2	1.706	$\bar{1}06$
40	2.543	9	2.561	122	20b	1.698	5	1.708	$2\bar{2}5$
		8	2.537	$0\bar{3}4$			2	1.706	$\bar{1}06$
		7	2.533	$\bar{1}04$			4	1.696	$\bar{4}20$
							3	1.694	410
30	2.481	4	2.466	$\bar{2}13$	30b	1.629	3	1.629	$1\bar{4}6$
							6	1.628	$\bar{4}\bar{1}4$
							2	1.627	$\bar{2}43$
							2	1.625	$\bar{1}60$
10	2.398	2	2.391	$2\bar{3}2$	10	1.608	4	1.617	340
30	2.315	2	2.316	$1\bar{4}3$	10	1.573	3	1.564	$\bar{2}56$
		2	2.315	$\bar{3}10$					
10	2.238	7	2.262	$0\bar{4}4$	10	1.459	2	1.463	$\bar{4}\bar{4}4$
		7	2.221	310					

*The 100% reflection in the calculated powder X-ray diffraction pattern at 10.0 Å could not be observed experimentally because the data capture range is below 9 Å.
**Calculated from structural data (Brandenburg and Putz, 2005).

Region, Chile (20°55′S 70°08′W). Associated minerals are halite, salammoniac, chanabayaite and joanneumite. The gabbro host rock consists of amphibole, plagioclase and minor clinochlore, and contains accessory chalcopyrite.

Antipinite forms imperfect, isometric and short prismatic crystals up to 0.1 mm × 0.1 mm × 0.15 mm in size, as well as their random aggregates up to 0.6 mm across (Fig. 1). The colour of the mineral is blue. The streak is pale blue, almost white. Crystals of antipinite are translucent, with a vitreous lustre. The mineral is brittle, with Mohs hardness of 2. Cleavage is medium in three directions; directions of cleavage could not be determined because of the absence of perfect crystals. Antipinite is non-fluorescent under UV. Density measured by flotation in heavy liquids is 2.53(3) g cm^{-3}. Density calculated from the empirical formula is 2.549 g cm^{-3}. Antipinite is optically biaxial (+), $\alpha = 1.432(3)$, $\beta = 1.530(1)$, $\gamma = 1.698(5)$, $2V_{meas} = 75(10)°$, $2V_{calc.} = 82°$. Dispersion is strong, $r < v$. Pleochroism is strong, blue on *Z*, light blue on *Y*, colourless on *X*; the absorption scheme is $Z > Y > X$.

In order to obtain an infrared (IR) absorption spectrum, a powdered sample of antipinite was mixed with dried KBr, pelletized and analysed using an ALPHA FTIR spectrometer (Bruker Optics) with a resolution of 4 cm^{-1} and 16 scans (Fig. 2). The IR spectrum of an analogous pellet of pure KBr was used as a reference. The assignment of absorption bands was made in accordance with Nyquist *et al*. (1996), Frost *et al*. (2003) and Frost (2004). Weak bands above 1800 cm^{-1} correspond to combination modes. Bands in the range 1500–1750 cm^{-1} correspond to asymmetric stretching vibrations of carboxylate groups and bands at 1280–1490 cm^{-1} correspond to their symmetric stretching vibrations. Bands at 780–900 cm^{-1} are assigned to in-plane bending vibrations of the carboxylate groups, possibly combined with C–C stretching vibrations. Bands from 495 to 557 cm^{-1} are assigned to out-of-plane bending vibrations of the carboxylate groups. No absorptions associated with H_2O molecules, C–H bonds, CO_3^{2-}, NO_3^- and OH^- ions are present in the IR spectrum. The IR spectrum of antipinite is unique and is considered as a good diagnostic tool for the mineral.

TABLE 3. Crystal parameters, data collection and structure refinement details for antipinite.*

Crystal data	
Formula	$KNa_3Cu_2(C_2O_4)_4$
Formula weight	587.2
Absorption, μ (mm^{-1})	3.228
Density, D_x (g cm^{-3})	2.546
Crystal system	Triclinic
Space group	$P\bar{1}$
a (Å)	7.1574(5)
b (Å)	10.7099(8)
c (Å)	11.1320(8)
α (deg)	113.093(1)
β (deg)	101.294(1)
γ (deg)	90.335(1)
V (Å^3)	766.5(1)
Z	2
Crystal size (mm)	0.10 × 0.15 × 0.15
Data collection	
Difractometer	SMART APEX2 CCD
Radiation; wavelength (Å)	Mo*K*α; 0.71073
Data collection method	ω
Temperature (K)	293
F(000)	572
Theta range for data collection (°)	2.04 to 33.67
Index ranges	$-11 < h < 11$ $-16 < k < 15$ $-16 < l < 17$
Reflections collected	11,361
Unique reflections / R_{int}	5553 / 2.63
Observed reflections, $I_{obs} > 2\sigma(I)$	4085
Refinement	
Refinement method	Full matrix least square on *F*
Weighting scheme:	$w = 1/(\sigma^2 F + 0.000529F^2)$
Goof on *F*	1.03
Final *R* indices	$R_1 = 3.27$; $wR_2 = 4.12$
$\Delta\rho_{min}$ / $\Delta\rho_{max}$ (e Å^{-3})	–0.49 / 0.33

*$R_1 = \sum||F_{obs}| - |F_{calc}||/\sum|F_{obs}|$; $wR_2 = \{\sum[w(F^2_{obs} - F^2_{calc})^2]/\sum[w(F^2_{obs})^2]\}^{1/2}$; Goof = $\{\sum[w(F^2_{obs} - F^2_{calc})]/(n-p)\}^{1/2}$ where *n* is the number of reflections and *p* is the number of refined parameters.

Chemical composition and chemical properties

Three electron microprobe analyses were carried out for Na, K and Cu using a VEGA TS 5130MM scanning electron microscope equipped with an EDX analyser (INCA Si(Li) detector), at an operating voltage of 20 kV and a beam current of 0.6 nA, beam rastered on an area 16 μm × 16 μm in order to minimize unstable sample damage. The program INCA Energy 200 was used for analytical data calculations. Attempts to use the wavelength dispersive spectroscopy mode with a higher beam current were unsuccessful because of the instability

TABLE 4. Fractional atom coordinates and equivalent isotropic displacement parameters (Å^2) for antipinite.

Site	*x*/*a*	*y*/*b*	*z*/*c*	U_{eq}
K1	–0.11025(6)	0.81681(5)	0.47781(5)	0.0205(2)
Cu1	0.38642(4)	0.83639(3)	0.47877(2)	0.0173(1)
Cu2	–0.21446(4)	0.53028(3)	0.56107(3)	0.0188(1)
Na1	–0.2311(1)	0.5411(1)	0.0532(1)	0.0188(3)
Na2	0.0193(1)	0.0982(1)	0.9013(1)	0.0247(3)
Na3	0.5392(1)	0.2206(1)	0.0123(1)	0.0256(3)
C1	0.3500(3)	0.0149(2)	0.7214(2)	0.0156(6)
C2	0.5679(3)	0.0080(2)	0.7266(2)	0.0151(6)
C3	0.4220(3)	0.6845(2)	0.2264(2)	0.0146(6)
C4	–0.0978(3)	0.7558(2)	0.7875(2)	0.0177(7)
C5	–0.2479(3)	0.4296(2)	0.2942(2)	0.0167(7)
C6	0.2047(3)	0.6904(2)	0.2229(2)	0.0165(7)
C7	–0.2117(3)	0.6558(2)	–0.1776(2)	0.0165(7)
C8	0.6467(3)	0.3217(2)	0.3239(2)	0.0188(7)
O1	0.5299(2)	0.7470(2)	0.3420(1)	0.0186(5)
O2	0.2418(2)	0.9507(2)	0.6052(2)	0.0197(5)
O3	–0.3478(3)	0.3520(2)	0.4486(2)	0.0253(6)
O4	0.1631(2)	0.7609(2)	0.3357(2)	0.0213(5)
O5	0.6816(2)	0.0751(2)	0.8316(2)	0.0204(5)
O6	–0.0899(2)	0.7120(2)	0.6636(2)	0.0215(5)
O7	0.0899(2)	0.6330(2)	0.1164(2)	0.0250(6)
O8	0.4768(2)	0.6271(2)	0.1214(2)	0.0196(5)
O9	0.2955(2)	0.0840(2)	0.8229(2)	0.0253(6)
O10	–0.1604(2)	0.5324(2)	0.3985(2)	0.0211(5)
O11	–0.2784(2)	0.5427(2)	0.7244(2)	0.0230(6)
O12	0.6111(2)	0.9347(2)	0.6151(2)	0.0195(5)
O13	–0.0240(3)	0.8656(2)	0.8756(2)	0.0273(6)
O14	–0.2483(2)	0.4105(2)	0.1784(2)	0.0229(6)
O15	0.5664(2)	0.2183(2)	1.2307(2)	0.0253(6)
O16	–0.2334(2)	0.6901(2)	–0.0624(2)	0.0217(6)

of the mineral. The contents of other elements with atomic numbers >8 are below detection limits. Carbon was measured using gas chromatography (CHN analysis) of the products by annealing at 1200°C with a Vario Micro cubeanalyser (Elementar GmbH, Germany). Hydrogen was not measured because of the absence of absorption bands for C–H bonds, H_2O molecules and OH^- groups in the IR spectrum. Analytical data are given in Table 1. The empirical formula (based on 16 O a.p.f.u.) is $K_{0.96}Na_{3.04}Cu_{2.03}(C_{2.00}O_4)_4$. The simplified formula is $KNa_3Cu_2(C_2O_4)_4$, which requires K 6.66, Na 11.74, Cu 21.64, C 16.36, O 43.59, total 99.99 wt.%. The Gladstone-Dale compatibility index is: $1 - (K_p/K_c) = 0.015$ ('superior'). Antipinite dissolves in water. A concentrated aqueous solution of antipinite has a pH of 9. An aqueous solution of the halite matrix without antipinite has a pH of 7. Tests with HCl and $BaCl_2$ show the absence of CO_3^{2-} and SO_4^{2-} groups. A test with sodium hexanitrocobaltate(III) solution confirms the presence of K.

X-ray diffraction data and crystal structure

Powder X-ray data were measured with Debye-Scherrer method (camera diameter 57.3 mm) using Cu*K*α radiation. The data are listed in Table 2. Unit-cell parameters refined from the powder data are $a = 7.17(2)$, $b = 10.73(2)$, $c = 11.17(2)$ Å, $\alpha = 113.07(6)$, $\beta = 101.29(5)$, $\gamma = 90.39(5)°$, $V = 771(2)$ Å^3. Single-crystal X-ray data were collected at room temperature with a Bruker SMART APEX2 CCD diffractometer (Bruker, 2009) with graphite monochromatized

TABLE 5. Anisotropic displacement parameters (Å^2) for antipinite.

Site	U^{11}	U^{22}	U^{33}	U^{12}	U^{13}	U^{23}
K1	0.0160(2)	0.0235(2)	0.0217(2)	–0.0009(2)	0.0060(2)	0.0079(2)
Cu1	0.0137(1)	0.0202(1)	0.0119(1)	–0.00115(9)	0.00452(9)	–0.0008(1)
Cu2	0.0280(2)	0.0144(1)	0.0120(1)	–0.0040(1)	0.0067(1)	0.00207(9)
Na1	0.0182(4)	0.0206(4)	0.0170(4)	–0.0014(3)	0.0054(3)	0.0061(3)
Na2	0.0188(4)	0.0307(5)	0.0200(4)	–0.0026(4)	0.0061(4)	0.0045(4)
Na3	0.0272(5)	0.0278(5)	0.0150(4)	–0.0029(4)	0.0051(4)	0.0013(4)
C1	0.0148(9)	0.0137(9)	0.0160(9)	–0.0013(7)	0.0055(7)	0.0026(7)
C2	0.0163(9)	0.0139(9)	0.0146(9)	0.0001(7)	0.0052(7)	0.0042(7)
C3	0.0139(9)	0.0140(9)	0.0148(9)	–0.0003(7)	0.0050(7)	0.0038(7)
C4	0.021(1)	0.0157(9)	0.0153(9)	0.0008(8)	0.0046(8)	0.0049(7)
C5	0.019(1)	0.0145(9)	0.0161(9)	0.0015(7)	0.0039(8)	0.0058(7)
C6	0.0154(9)	0.0172(9)	0.0147(9)	–0.0006(7)	0.0041(7)	0.0036(7)
C7	0.019(1)	0.0159(9)	0.0137(9)	0.0012(7)	0.0055(8)	0.0046(7)
C8	0.023(1)	0.0161(9)	0.0159(9)	–0.0013(8)	0.0036(8)	0.0058(8)
O1	0.0123(7)	0.0245(8)	0.0125(7)	–0.0003(6)	0.0023(5)	0.0008(6)
O2	0.0122(7)	0.0234(8)	0.0149(7)	–0.0014(6)	0.0024(5)	–0.0009(6)
O3	0.040(1)	0.0180(7)	0.0141(7)	–0.0109(7)	0.0065(7)	0.0027(6)
O4	0.0145(7)	0.0273(8)	0.0132(7)	–0.0009(6)	0.0043(6)	–0.0018(6)
O5	0.0174(7)	0.0217(8)	0.0157(7)	–0.0009(6)	0.0015(6)	0.0017(6)
O6	0.0316(9)	0.0163(7)	0.0140(7)	–0.0043(6)	0.0072(6)	0.0024(6)
O7	0.0162(7)	0.0348(9)	0.0153(7)	–0.0027(7)	0.0013(6)	0.0018(7)
O8	0.0185(7)	0.0213(7)	0.0149(7)	–0.0003(6)	0.0069(6)	0.0015(6)
O9	0.0206(8)	0.0275(8)	0.0173(8)	–0.0029(6)	0.0093(6)	–0.0042(6)
O10	0.0311(9)	0.0165(7)	0.0133(7)	–0.0055(6)	0.0068(6)	0.0026(6)
O11	0.0340(9)	0.0174(7)	0.0153(7)	–0.0061(6)	0.0101(7)	0.0020(6)
O12	0.0161(7)	0.0227(8)	0.0135(7)	–0.0006(6)	0.0058(6)	–0.0005(6)
O13	0.041(1)	0.0174(7)	0.0173(8)	–0.0073(7)	0.0081(7)	–0.0001(6)
O14	0.0322(9)	0.0230(8)	0.0125(7)	–0.0046(7)	0.0044(6)	0.0063(6)
O15	0.0346(9)	0.0195(8)	0.0167(7)	–0.0075(7)	0.0019(7)	0.0037(6)
O16	0.0273(8)	0.0236(8)	0.0142(7)	0.0018(6)	0.0088(6)	0.0055(6)

Mo$K\alpha$ radiation ($\lambda = 0.71073$ Å) and a CCD detector using the ω scanning mode. The following triclinic unit-cell parameters were obtained by least-squares refinement: $a = 7.1574(5)$, $b = 10.7099(8)$, $c = 11.1320(8)$ Å, $\alpha = 113.093(1)$, $\beta = 101.294(1)$, $\gamma = 90.335(1)°$, $V = 766.5(1)$ Å^3, space group $P\bar{1}$. A total of 11,361 reflections within the sphere limited by $\theta = 33.67°$ were measured. Raw data were integrated using the program *SAINT* and then scaled, merged and corrected for Lorentz-polarization effects using the *SADABS* package. The experimental details of the data collection and refinement results are listed in Table 3. The initial structure model was determined by the 'charge-flipping' method (Palatinus and Chapuis, 2007) and refined to $R = 3.27\%$ [4085 $I > 2\sigma(I)$] in the anisotropic approximation using the crystallographic program *Jana2006* (Petricek *et al*., 2006). Final atom parameters are shown in Tables 4 and 5. Interatomic distances are presented in Table 6.

The structure of antipinite consists of planar C_2O_4 units, a layer of sodium atoms and a layer of Cu atoms with pairs of K atoms (Fig. 3). Both layers are coplanar with the (001) plane and are joined by an O atom shared with oxalate groups. There are eight independent oxalate groups with bond lengths C–O and C–C in the ranges 1.219–1.288 and 1.551–1.560 Å, respectively. The Cu atoms Cu1 and Cu2 are coordinated to two oxalate groups with orthogonal disposition of CuO_4 planes (Fig. 4*a*). The Cu-centred polyhedra are square bipyramids with two O atoms forming long Cu–O bonds (Table 6, Fig. 4*b*). Thus the coordination

TABLE 6. Interatomic distances (Å) in the crystal structure of antipinite.

K1	O1	2.654(1)	Na3	O9	2.395(2)
	O4	2.678(2)		O14	2.404(2)
	O6	2.696(2)		O15	2.411(2)
	O2	2.717(1)		O5	2.424(2)
	O12	2.760(2)		O16	2.470(2)
	O10	2.818(2)		O8	2.593(2)
	O2	3.071(2)	Mean		2.450
Mean		2.771			
Cu1	O4	1.929(1)		Oxalate group 1	
	O12	1.941(1)	C1–O9		1.223(3)
	O1	1.942(2)	C1–O2		1.285(2)
	O2	1.945(2)	C1–C2		1.553(3)
	O3	2.482(2)	C2–O5		1.227(2)
	O12	3.019(2)	C2–O12		1.282(3)
Mean		2.210			
Cu2	O11	1.916(2)		Oxalate group 2	
	O6	1.930(1)	C3–O8		1.232(3)
	O10	1.932(2)	C3–O1		1.277(2)
	O3	1.939(2)	C3–C6		1.550(3)
	O10	2.764(2)	C6–O7		1.225(2)
	O3	3.382(2)	C6–O4		1.281(3)
Mean		2.311			
Na1	O14	2.347(2)		Oxalate group 3	
	O7	2.354(2)	C4–O13		1.228(2)
	O16	2.410(2)	C4–O6		1.284(3)
	O8	2.427(2)	C4–C7		1.550(4)
	O8	2.448(1)	C7–O16		1.230(3)
	O7	2.464(2)	C7–O11		1.280(2)
Mean		2.408			
Na2	O9	2.295(2)		Oxalate group 4	
	O13	2.352(2)	C5–O14		1.223(3)
	O5	2.369(2)	C5–O10		1.287(2)
	O13	2.404(2)	C5–C8		1.550(4)
	O16	2.530(2)	C8–O15		1.221(2)
Mean		2.390	C8–O3		1.288(3)

(4+2) of Cu1 and Cu2 ions corresponds to the most common type (Burns and Hawthorne, 1995, 1996; Krivovichev *et al*., 2013) where apical ligands are further from the central atom due to the Jahn-Teller effect. The Cu2 bipyramid is connected via common edges to form columns running along the *a* axis which are combined into a layer by pairs of the Cu1 bipyramid (Fig. 4). Potassium atoms occupy large loops in the Cu layer. Each Na atom is coordinated with O atoms of the oxalate groups. The $Na1O_6$ and $Na3O_6$ polyhedra are distorted octahedra and are combined in bands. The Na2 atom is five-coordinate and these polyhedra connect bands via common edges to form a layer (Fig. 5).

Discussion

Antipinite is the 19th mineral containing the oxalate anion, $C_2O_4^{2-}$. Other copper oxalates known in Nature are moolooite, $Cu(C_2O_4)\cdot nH_2O$ ($n < 1$) and wheatleyite, $Na_2Cu(C_2O_4)_2\cdot 2H_2O$. No minerals or synthetic compounds related to antipinite in terms of crystal structure are known. Crystallographic data for Cu oxalates compounds are summarized in Table 7. The crystal structure of the synthetic analogue of wheatleyite, $Na_2Cu(C_2O_4)_2\cdot 2H_2O$ (Gleizes *et al*., 1980; Fig. 6), consists of columns of Cu-centred octahedra running along the *a* axis ($a = 3.6$ Å) and corrugated layers of seven-coordinate Na-centred polyhedra

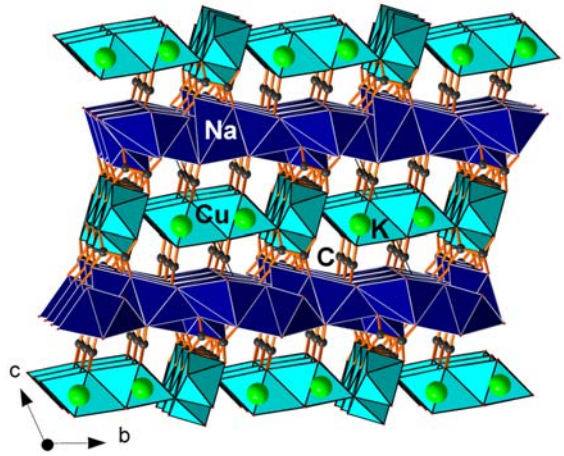

FIG. 3. General view of the antipinite structure projected on (100). The orange lines indicate C–O bonds.

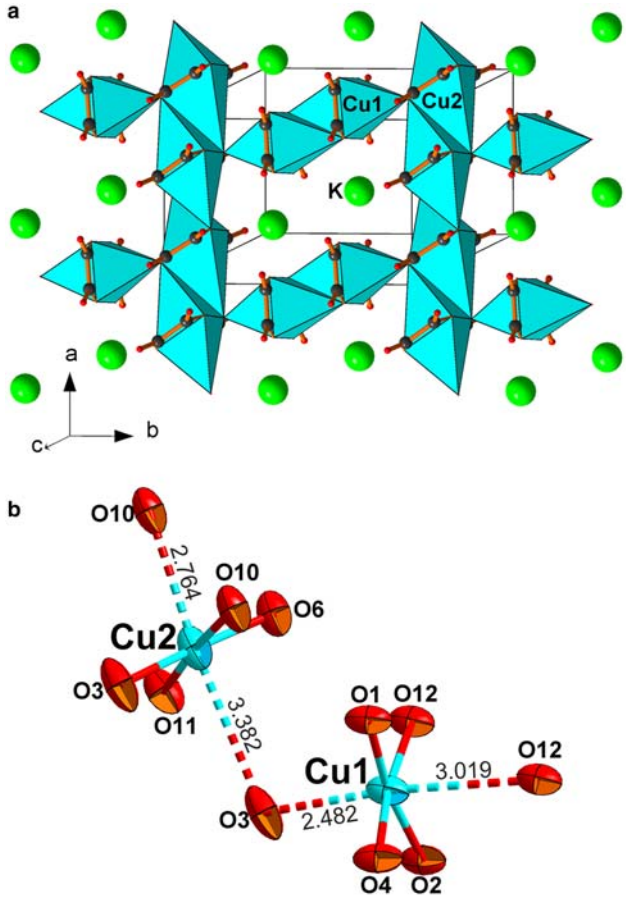

FIG. 4. Layer of Cu-centred bipyramids in the structure of antipinite (*a*) and a representation of high Jahn-Teller distortion of Cu-polyhedra (*b*).

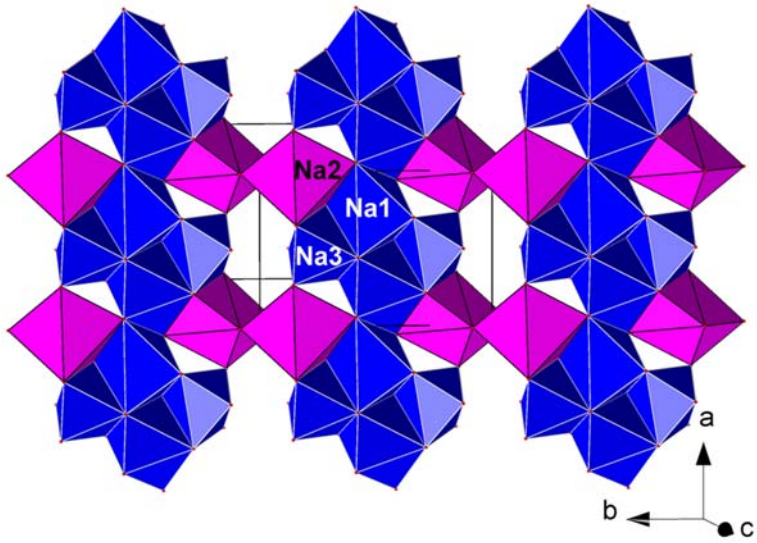

FIG. 5. Layer of Na-centred polyhedra in the structure of antipinite.

TABLE 7. Crystallographic data for natural and synthetic copper oxalates.

Mineral / Compound	Space group, Z	Unit-cell parameters a, Å; b, Å; c, Å; α, °; β, °; γ, °	References*
Moolooite, $Cu(C_2O_4)\cdot nH_2O$ ($n = 0.4$–0.7)	*Pnnm*, 1	5.381–5.348; 5.625–5.639; 2.548–2.559	1, 2, 3
$Cu(C_2O_4)\cdot 3H_2O$	*Pcca*, 4	9.760; 6.603; 10.500	4
$Cu(C_2O_3OH)_4\cdot 8H_2O$	$P\bar{1}$, 1	6.947; 8.900; 9.045 107.371; 98.029; 96.476	5
Wheatleyite, $Na_2Cu(C_2O_4)_2\cdot 3H_2O$	$P\bar{1}$, 1	7.536; 9.473; 3.576 81.9; 103.77; 108.09	6
$Na_2Cu(C_2O_4)_2\cdot 2H_2O$	$P\bar{1}$, 1	3.583; 9.649; 7.549 109.07; 76.38; 103.32	8
Antipinite, $KNa_3Cu_2(C_2O_4)_4$	$P\bar{1}$, 2	7.157; 10.710; 11.132 113.093; 101.294; 90.335	This work
$K_2Cu(C_2O_4)_2\cdot 4H_2O$	$P2_1/n$, 2	3.777; 14.819; 10.756 93.18	9
$Rb_2Cu(C_2O_4)_2\cdot 2H_2O$	$P\bar{1}$, 2	7.000; 8.949; 8.982 108.05; 97.69; 97.99	10
$Sr_2Cu(C_2O_4)_3\cdot 7H_2O$	$P\bar{1}$, 2	6.349; 10.258; 15.737 73.21; 93.66; 76.44	11
$Cs_2Cu(C_2O_4)_2\cdot 2H_2O$	$P\bar{1}$, 2	9.298; 9.117; 7.132 97.524; 97.410; 107.522	12
$BaCu(C_2O_4)_2\cdot 6H_2O$	$P\bar{1}$, 2	9.209; 10.938; 6.547 100.83; 99.65; 85.45	13, 14, 15

*References: 1, Clarke and Williams (1986); 2, Chisholm *et al*. (1987); 3, Schmittler (1968); 4, Wu and Zhai (2007); 5, Yesilel *et al*. (2010); 6, Rouse *et al*. (1986); 7, Gleizes *et al*. (1980); 8, Chananont *et al*. (1980); 9, Jian *et al*. (2001); 10, Kolitsch (2004); 11, Insausti *et al*. (1994); 12, Pannhorst and Löhn (1974); 13, Hallock, *et al*. (1990); 14, Bouayad *et al*. (1995); 15, Kasthuri *et al*. (1996).

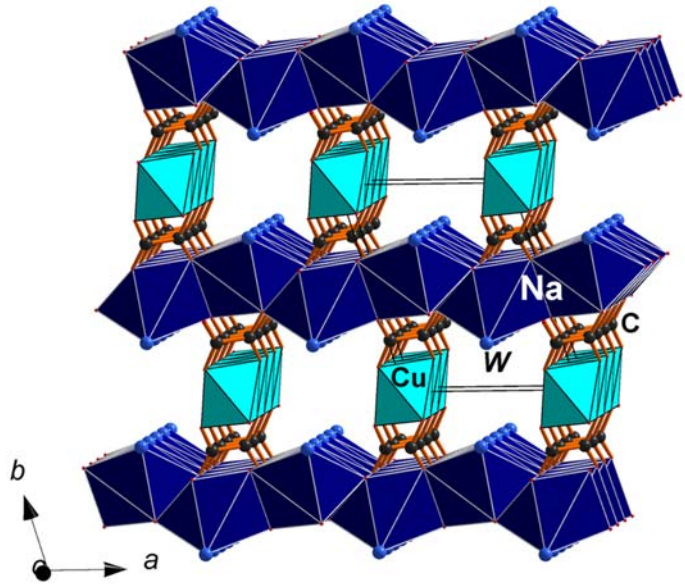

FIG. 6. The crystal structure of wheatleyite.

perpendicular to the *b* axis ($b = 9.5$ Å). The columns and the layers in wheatleyite are combined by oxalate anions and H bonds of water molecules in the vertices of Na-centred polyhedra.

Antipinite is a supergene mineral formed in the contact zone between a deeply altered guano deposit and chalcopyrite-bearing gabbro. Guano was the source of oxalate groups, and oxidized chalcopyrite was the source of Cu for antipinite and associated chanabayaite and joanneumite (Bojar and Walter, 2012; Chukanov *et al*., 2013).

Antipinite is the only known anhydrous Cu oxalate compound and the only one that simultaneously contains Na and K.

Acknowledgements

This study was supported by the Russian Scientific Foundation grants 14-17-00048 (characterization excluding XRD and crystal structure) and 14-17-00071 (X-ray diffraction studies and crystal structure). The authors are grateful to P. Leverett, I. Grey and M.J. Sciberras for reviewing the paper and for their helpful comments and corrections.

References

Appleton, J.D. and Notholt, A.J.G. (2002) Local phosphate resources for sustainable development of Central and South America. *British Geological Survey Economic Minerals and Geochemical Baseline Programme Report*, CR/02/122/N. BGS, Keyworth, Nottingham, UK.

Bojar, H.-P. and Walter, F. (2012) Joanneumite, IMA 2012-001. CNMNC Newsletter No. 13, June 2012, 814; *Mineralogical Magazine*, **76**, 807–817.

Bojar, H.-P., Walter, F., Baumgartner, J. and Färber, G. (2010) Ammineite, $CuCl_2(NH_3)_2$, a new species containing an ammine complex: mineral data and crystal structure. *The Canadian Mineralogist*, **48**, 1359–1371.

Bouayad, A., Trombe, J.C. and Gleizes, A. (1995) Barium-copper(II) oxocarbon compounds: synthesis, crystal structures and thermal behaviours of $[Ba(H_2O)_5][Cu(C_2O_4)_2(H_2O)]$ and $[Ba(C_4O_4)_{0.5}(H_2O)_2]_2[Cu(C_4O_4)_2(H_2O)_2]$. *Inorganica Chimica Acta*, **230**, 1–7.

Brandenburg, K. and Putz, H. (2005) *DIAMOND Version 3*. Crystal Impact GbR, Bonn, Germany.

Bruker (2009) *APEX2*. Bruker AXS Inc., Madison, Wisconsin, USA.

Burns, P.C. and Hawthorne, F.C. (1995) Coordination-geometry structural pathways in Cu^{2+} oxysalt minerals. *The Canadian Mineralogist*, **33**, 889–905.

Burns, P.C. and Hawthorne, F.C. (1996) Static and dynamic Jahn-Teller effects in Cu^{2+} oxysalt minerals. *The Canadian Mineralogist*, **34**, 1089–1105.

Chananont, P., Nixon, P.E., Waters, J.M. and Waters, T.N. (1980) The structure of disodium *catena-bis*(μ-oxalato)-cuprate dehydrate. *Acta Crystallographica*, **B36**, 2145–2147.

Chisholm, J.E., Jones, G.C. and Purvis, O.W. (1987) Hydrated copper oxalate, moolooite, in lichens. *Mineralogical Magazine*, **51**, 715–718.

Chukanov, N.V., Zubkova, N.V., Möhn, G., Pekov, I.V., Zadov, A.E and Pushcharovsky, D.Y. (2013) Chanabayaite, IMA 2013-065. CNMNC Newsletter No. 17, October, 2013, p. 3004; *Mineralogical Magazine*, **77**, 2997–3005.

Chukanov, N.V., Aksenov, S.M., Rastsvetaeva, R.K., Lysenko, K.A., Belakovskiy, D.I., Färber, G. and Van, K.V. (2014*a*) Antipinite, IMA 2014-027. CNMNC Newsletter No. 21, August 2014, page 837; *Mineralogical Magazine*, **78**, 833–840.

Chukanov, N.V., Britvin, S.N., Möhn, G., Pekov, I.V., Zubkova, N.V., Nestola, F., Kasatkin, A.V. and Dini, M. (2014*b*) Shilovite, IMA 2014-016. CNMNC Newsletter No. 21, October 2014, page 798; *Mineralogical Magazine*, **78**, 797–804.

Clarke, R.M. and Williams, I.R. (1986) Moolooite, a naturally occurring hydrated copper oxalate from Western Australia. *Mineralogical Magazine*, **50**, 295–298.

Ericksen, G.E. (1981) Geology and origin of the Chilean nitrate deposits. *United States Geological Survey Professional Paper*, **1188**. USGS, Washington DC.

Frost, R.L. (2004) Raman spectroscopy of natural oxalates. *Analytica Chimica Acta*, **517**, 207–214.

Frost, R.L., Yang Jing and Zhe Ding (2003) Raman and FTIR spectroscopy of natural oxalates: implications for the evidence of life on Mars. *Chinese Science Bulletin*, **48**, 1844–1852.

Gleizes, A., Maury, F. and Galy, J. (1980) Crystal structure and magnetism of sodium *bis*(oxalato)cuprate(II) dihydrate, $Na_2Cu(C_2O_4)_2\cdot 2H_2O$. A deductive proposal of the structure of copper oxalate, $Cu(C_2O_4)\cdot xH_2O$ ($0 < x < 1$). *Inorganic Chemistry*, **19**, 2074–2078.

Hallock, R.B., Rhine, W.E., Cima, M.J., Bott, S.G. and Atwood, J.L. (1990) Synthesis and X-ray crystal structure of $BaCu(C_2O_4)_2\cdot 6H_2O$, a mixed-metal oxalate of barium and copper. *Superconductivity and Ceramic Superconductors II (Ceramic Transactions)*, **13**, 251–258.

Insausti, M., Urtiaga, M.K., Cortes, R., Mesa, J.L. and Arriortua, M.I. (1994) Synthesis, crystal structure and properties of $Sr_2Cu(C_2O_4)_3(H_2O)_7$: precursor of Sr_2CuO_3 oxide. *Journal of Materials Chemistry*, **4**, 1867–870.

Jian, F., Wei-Yin, S., Okamura, T., Kai-Bei, Y. and Ueyama, N. (2001) The X-ray crystal structural characterization of dipotassium bisoxalato copper(II) tetrahydrate, $[K_2Cu(ox)_2\cdot 4H_2O]$ (*ox* = oxalate dianion). *Inorganica Chimica Acta*, **319**, 240–246.

Kasthuri, V.B., Rao, P.M. and Nethaji, M. (1996) The crystal structure of hydrated barium copper oxalate. *Crystal Research and Technology*, **31**, 287–294.

Kolitsch, U. (2004) $RbCr(III)(C_2O_4)_2\cdot 2H_2O$, $Cs_2Mg(C_2O_4)_2\cdot 4H_2O$ and $Rb_2Cu(II)(C_2O_4)_2\cdot 2H_2O$: three new complex oxalate hydrates. *Acta Crystallographica*, **C60**, m129–m133.

Krivovivhev, S.V., Filatov, S.K. and Vergasova, L.P. (2013) The crystal structure of ilinskite, $NaCu_5O_2(SeO_3)_2Cl_3$, and review of mixed-ligand CuO_mCl_n coordination geometries in minerals and inorganic compounds. *Mineralogy and Petrology*, **107**, 235–242.

Nyquist, R.A., Putzig, C.L. and Leugers, M.A. (1996) *Handbook of Infrared and Raman Spectra of Inorganic Compounds and Organic Salts.* Vol. 3, Academic Press, New York.

Palatinus, L. and Chapuis, G. (2007) SUPERFLIP – a computer program for the solution of crystal structures by charge flipping in arbitrary dimensions. *Journal of Appied Crystallography*, **40**, 786–790.

Pankhurst, R.J. and Hervé, F. (2007) Introduction and overview. Pp. 1–4 in: *The Geology of Chile* (T. Moreno and W. Gibbons, editors). The Geological Society, London.

Pannhorst, W. and Löhn, J. (1974) Die Kristallstruktur von Caesium-Kupfer(II)–Oxalat–Dihydrat, $Cs_2Cu(C_2O_4)_2\cdot 2H_2O$. *Zeitschrift für Kristallographie*, **139**, 236–245.

Petricek, V., Dusek, M. and Palatinus, L. (2006) *Jana2006. Structure Determination Software Programs*. Institute of Physics, Praha, Czech Republic.

Rouse, R.C., Peacor, D.R., Dunn, P.J., Simmons, W.B. and Newbury, D. (1986) Wheatleyite, $Na_2Cu(C_2O_4)_2\cdot 2H_2O$, a natural sodium copper salt of oxalic acid. *American Mineralogist*, **71**, 1240–1242.

Schmittler, H. (1968) Structural principle of disordered copper(II) oxalate $CuC_2O_4\cdot nH_2O$. *Monatsberichte der Deutschen Akademie der Wissenschaften zu Berlin*, **10**, 581–604.

Wu, W.-Y. and Zhai, L. (2007) Poly[diaqua-μ-oxalato-copper(II) monohydrate]. *Acta Crystallographica.* **E63**, m567–m568.

Yesilel, O.Z., Erer, H., Odabasoglu, M. and Buyukgungor, O. (2010) A novel copper(II)-hydrogen oxalate coordination polymer showing a new coordinate mode. *Journal of Inorganic and Organometallic Polymers*, **20**, 78–82.